MULTIFUNCTIONAL FINGERPRINTING OF INDIVIDUAL FIBROBLASTS USING MEMS-BASED DEVICES

Ji Chang[1], Omar Cepeda-Torres[1], Saqib Shahzad[1], Guntis Rutins[1], Richard G. Blair[1], Swaminathan Rajaraman[1] and Laurene Tetard[1,2]*

[1]University of Central Florida, Orlando, FL, USA

[2]Universite Claude Bernard Lyon 1, ISA, UMR5280, CNRS, Villeurbanne, FRANCE

ABSTRACT

Single cell analysis is essential to explore the variability of physical and chemical properties in cell populations in view of revealing new signatures associated with early signs of diseases or uncharted cellular processes. The complexity of microfluidic devices and tools needed to access the information at a cellular level can hinder progress in single cell analysis. Here we propose a novel method exploiting the versatility of atomic force microscopy to determine the morphology, mechanical properties, infrared fingerprint, and electrical impedance on single cells. The approach is used to identify the differences between untreated and ultraviolet light (UV) treated fibroblasts.

KEYWORDS

Atomic Force Microscopy, Nanoscale Infrared Spectroscopy, Nanomechanical measurements, Electrical Impedance Spectroscopy (EIS), Single cell Analysis, Ultraviolet Light Treatment

INTRODUCTION

Great strides in single cell analyses have been reported using sequencing technologies facilitated by microfluidics and nanotechnology **[1]**. Even with the emergence of multimodal and integrative sequencing-based methods that make it possible to study intracellular and membrane proteins, DNA, mRNA or genomic profiles **[1-3]**, the understanding of biomolecular interactions in the cell and their relationship to cellular functions is still lagging.

To monitor cellular responses to external stimuli or stresses resulting from the molecular changes at the single cell level detected by sequencing-based techniques, high spatial resolution and sensitivity are required. Atomic force microscopy (AFM) is a versatile tool that has been extensively used to study biological systems, including cells and bacteria, in dry state and aqueous media **[4, 5]**. As AFM reconstructs images of the sample based on the force measured between the nanoscale AFM tip and the sample, it is possible to access a rich library of information by simply modifying the nature of the tip and/or the experimental conditions to create a regime in which a given force is predominant. For instance, it is possible to apply a force to locally deform the cell, so as to determine its mechanical properties **[6, 7]**. It is also possible to functionalize the AFM tip with a charged chemical group, a DNA strand, or a protein to determine the affinity of the selected molecule with various entities of the cells **[8, 9]**. Other properties of cells have been investigated with different modes of AFM, including their composition **[10]**, electrical properties **[11]**, and electrochemical processes at their surfaces **[12]**.

Sensors have also been developed for single cell analysis, using microfluidic devices and fabricated chips to carry out electrical measurements. High-cost fabrication of these chips and the requirement for skilled labor to perform and interpret the electrical measurements can hinder the implementation of single cell analysis tools in clinical settings **[1]**. However, complementing the electrical analysis of the cell with orthogonal information such as morphology, composition and mechanical properties has the potential to improve the understanding of the electrical data. Herein we present a multi-functional fingerprinting of individual cells obtained using orthogonal measurements carried out with MEMS-based microcantilevers. The information collected on the morphology, composition, and mechanical properties of the cells with AFM functional modes is expected to guide the understanding of impedance signatures acquired with a novel electrode design consisting of two custom-printed high aspect ratio carbon microelectrodes for single cell analysis. The approach is implemented to compare the multi-functional profiling of untreated cells and cells treated by ultraviolet (UV) light, which is expected to lead to apoptosis.

MATERIALS AND METHODS

Cell Culture

Immortalized mouse fibroblast NIH3T3 were plated on 22 mm × 22 mm square-cut silicon substrates and maintained with a medium containing 90% Dulbecco Modified Eagle Medium (DMEM) and 10% Fetal Calf Serum (FCS). The cells were then left inside an incubator regulated at 37 °C with 5% carbon dioxide (CO_2) overnight. Next, the cells were treated by exposure to UV light (254 nm) for 0 min (untreated control) and 1 h. After UV exposure, the cells were fixed with cold 4% paraformaldehyde before being placed in the incubator for 15 min to set. Afterwards, the cells were rinsed thoroughly three times using phosphate buffer solution (PBS). Finally, the wells were filled with PBS, wrapped in parafilm and aluminum foil, and stored in a 4 °C refrigerator.

Sample Preparation

The cells were washed thoroughly with a mixture of phosphate buffer solution at a pH of 7.4 and ultrapure water. The substrate was then tilted at an angle in the well and set to air dry. After the sample was fully dried, it was covered using parafilm until imaging. Live cells were rinsed and immediately transferred for measurements.

Topography Imaging with Atomic Force Microscopy (AFM)

AFM uses a microcantilever with a nanoscale tip scanning over the sample surface to reveal different characteristics of the sample with nanoscale resolution. The cell sample was attached to an AFM metallic disk using tape and placed on the sample holder. To determine the morphology of the cells, the topography images were recorded in tapping mode with constant amplitude feedback using a FORTGG cantilever (AppNano). The first resonance frequency of the cantilever was used ($f_{res} \sim 60$ kHz) and the phase was zeroed during the frequency tuning process. The sample height and phase images were recorded with 512 points × 512 points. The thickness and diameter of the cells were extracted from the height images.

978-1-940470-05-4/HH2024/$25©2024TRF
DOI 10.31438/TRF.HH2024.84

AFM Nanomechanical Measurements

Force curves were recorded at selected points across each cell. Here three force curves per nucleus were analyzed to compare the mechanical properties of the untreated and UV treated cells (N=7). The tip-sample distance was varied until the free cantilever contacted the cell surface during the approach. A maximum force (or peak force) corresponding to deflection increase of 0.25 V compared to the deflection of the free cantilever was applied during the approach curve. Once the peak force was reached, the cantilever was withdrawn away from the sample surface until it was no longer contacting the cell. The deflection sensitivity of the cantilever was determined by acquiring a force curve on a non-deformable sapphire substrate with the same cantilever. The cantilever spring constant k was determined by thermal tuning. Both were used to transform the deflection signal in Volts into a force measurement in Newtons.

Atomic Force Microscopy Infrared Spectroscopy (AFM-IR)

AFM-IR uses infrared light (Daylight MIRCat QCL laser) to excite molecular vibrations in the cell, which leads to photothermal expansion that can be detected mechanically by the AFM cantilever. AFM-IR spectra were acquired in contact mode. PLL tracking was used to monitor the amplitude of the evolving contact resonance. The IR laser was aligned to illuminate the region underneath the AFM tip. The laser pulse was swept to match the contact resonance of the cantilever. This was performed at an illumination wavenumber absorbed by the cell to generate photothermal expansion that can be measured by the cantilever. Once the cantilever resonance and laser pulse width were set, a background spectrum was collected using an infrared photodetector to determine the profile of the IR laser emission in the 1800-900 cm^{-1} range. An array of AFM-IR spectra (at least 25 spectra per cell) was collected across each image in hyperspectral mode to allow for spatial reconstruction of the chemical maps. Savitzky-Golay smoothing (15 pts) was used for spectral analysis and display. Each spectrum represents the amplitude of the cantilever contact resonance as a function of wavenumber.

Carbon Rods Cantilever Set-Up and Impedance Measurements

The carbon microrods with high aspect ratios were 3D printed following the process recently reported by Torres Davila et al. **[13]**. In short, an engineered hexagonal boron nitride catalyst was pressurized in a hydrocarbon gas sealed in a custom photoreactor. Carbon growth was initiated by illuminating the catalyst with a visible laser (532 nm, ~ 10 mW) focused on the surface of the catalyst with a 10× objective. The high aspect ratio of the rod was obtained by moving the focus of the light in concert with the tip of the carbon structure during growth. The growth was stopped by turning the light off. Carbon microrods were manually isolated and positioned on a silicon chip compatible with the AFM cantilever mount. This design was utilized to take advantage of the high precision of the AFM stage. The two-electrode system was used in place of the AFM microcantilever and positioned above the individual cells using the optical view of the system. The optical view was used to approach the carbon rods in contact with the cell surface, which was confirmed by a change in deflection of the rods. Each carbon microrod was electrically connected using conductive carbon paint. For EIS, the electrode was connected to the Bode impedance analyzer set in series-through mode.

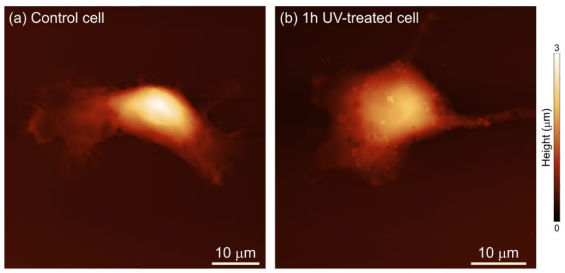

Figure 1: AFM topography images of (a) a control fibroblast and (b) a UV-treated fibroblast.

The impedance measurements were carried out three times on each cell, for three cells of each treatment.

RESULTS

Effect of the UV-treatment on cell morphology

AFM height images of fixed and dried cells confirmed a clear difference in shape between untreated control and UV treated cells, also visible with optical imaging. As shown in **Figure 1(a)**, most control cells exhibited features suggesting the expansion of the cell in one direction (~ 40 µm in the elongated direction compared to ~ 12 µm in the other direction) with a protruding nucleus region (~ 3 µm in height). A high number of apoptotic cells were found after the UV treatment. They displayed rounder cell morphology (15-20 µm in diameter) as shown in **Figure 1(b)**. A small change in height was observed with a thickness of ~ 2 µm in the cell presented here, though we note that height variability of the cells was challenging to quantify due to the heterogeneities found in each cell and each sample group.

Effect of the UV-treatment on cell nanomechanics

The mechanical properties of the cells were evaluated by acquiring an array of force curves on several cells of each group. The slope of the region of the withdraw curve from the peak force position (minimum distance between the tip and the sample) to the pull-out of contact position was calculated for each point. **Figure 2** presents the comparison of the slopes measured at selected points above the nucleus of the cells. The slope of the control cells was found to have a mean value of about -0.013 V/nm, while the slopes of the treated cells exhibited a mean value of about -0.014 V/nm, suggesting that the **UV treatment deteriorates the cell is such a way that its stiffness increases**.

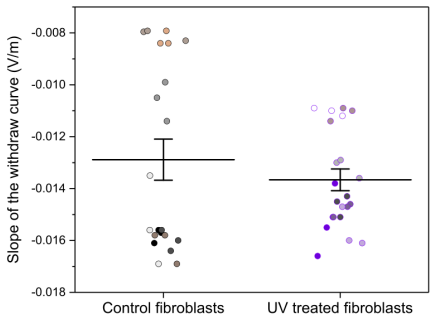

Figure 2: Comparison of the mechanical deformation of the cells determined by AFM force curve measurements (N=7). Each group of color corresponds to the measurements extracted from the same cell. Horizontal lines represent the mean value of the data.

However, we note that the variability observed from cell to cell within each group could be attributed to apoptotic cells in the control sample (for instance due to sample preparation steps) or cells in the UV treated samples that did not yet reach the apoptotic regime. Another source of error is the selection of the points in the regions of the nucleus, which can be hard to distinguish from the topography images alone. A more comprehensive statistical analysis of the all the force curves collected for a larger number of cells should be considered to alleviate these limitations, which is out of the scope of this work.

Effect of UV-treatment on cellular composition

Nanoscale infrared spectra were acquired across the cells as a hyperspectral image. This approach allowed to prevent damaging the cells and provided a way to reconstruct the chemical map of the cell at different wavenumbers.

In **Figure 3**, we present the topography images of the control (**Figure 3(a)**) and UV-treated cells (**Figure 3(b)**) and corresponding chemical representation (**Figure 3(c) and (d)**, respectively). The chemical representation of the cells was constructed by integrating the spectrum in regions P1 and P2, as marked in **Figure 3 (e, f)**, followed by calculating the ratio of the two values P1/P2.

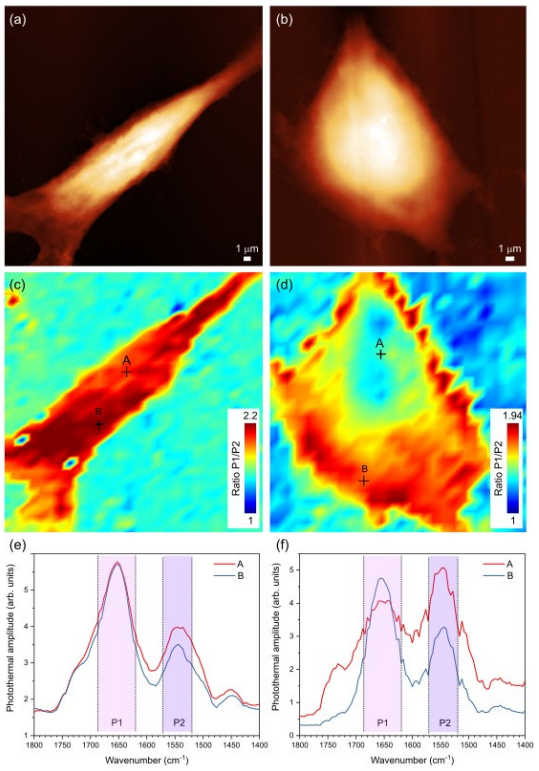

Figure 3: Comparison of the composition of the fibroblasts before and after UV-treatment. (a) AFM topography image of the control fibroblasts. (b) AFM topography image of the UV-treated fibroblasts. (c) Nanoscale infrared representation of the control fibroblasts. (d) Nanoscale infrared representation of the UV-treated fibroblasts.(e) Nanoinfrared spectra acquired on the nucleus and cytoplasm regions of the control fibroblast. (e) Nanoinfrared spectra acquired on the nucleus and cytoplasm regions of the UV-treated fibroblast.

This provided a measure of the relative change in Amide 1 (centered at ~ 1660 cm^{-1}) and Amide 2 (centered at ~ 1540 cm^{-1}) bands, which revealed a **critical change in the signal collected when the tip was on top of the nucleus after UV treatment.** The ratio measured in this region decreased from ~2 in the control cells to ~1 after UV treatment. Inspection of the individual spectra revealed that the change in ratio originates from both a change in the intensity of the Amide 1 and Amide 2 bands. This is indicative of a change in the secondary structure of the proteins, specifically in the region of the nucleus. In addition, the spectra acquired on the nucleus of the UV treated cell exhibit a stronger IR band centered ~ 1740 cm^{-1}, corresponding to the stretching of C=O ester in lipids. This is consistent with observations made in the infrared spectra of apoptotic yeast and cells **[14, 15]**.

Electrical Measurements on Single Cells

Carbon rods with high aspect ratios (diameter ~5-10 µm and length from 1 to 2 mm, corresponding to aspect ratios of 100-400) were produced as described in the Methods **[13]**. **Figure 4** shows a scanning electron microcopy (SEM) image of a representative carbon rod extracted from the reactor before positioning on the silicon chip for electrical measurements.

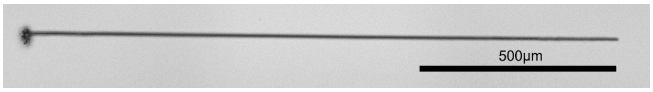

Figure 4: SEM image of a carbon rod grown according to the method reported by Torres Davila et al. [13] and transferred on sapphire for imaging.

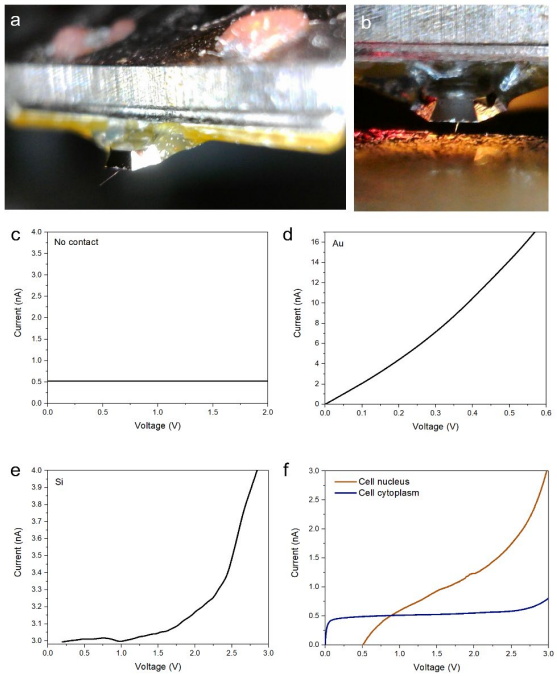

Figure 5: Carbon rods used as a single electrode to acquire I-V curves. (a, b) Optical views of the carbon microelectrodes held on an AFM cantilever holder away from the surface (a) and in contact with the sample surface (b). (c-f) I-V curves collected on different materials with the microelectrode (c) away from the surface, and in contact with (d) gold, (e) silicon, (f) a fixed mammalian cell nucleus and cytoplasm.

We first evaluated the carbon microrod as an electrode for electrical measurements. We placed the carbon rod on a silicon chip as shown in **Figure 5(a, b)**, and connected it to the electrical circuit using conductive carbon paint. Next, we approached the electrode to the surface of several materials, including gold (Au), silicon (Si) and a fixed and dry fibroblast. In each case, sample was grounded, and the bias applied to the tip was swept from 0 to 2V. The resulting current was measured. I-V plots corresponding to each case are presented in **Figure 5(c-f)**. The profiles expected for a metal **(Figure 5(d))** and a semiconductor **(Figure 5(e))** were obtained, suitable for qualitative comparison. **Measurements acquired at different points of the cells resulted in different I-V curves, the nucleus providing better conductivity than the cytoplasm (Figure 5(f)).**

The next steps consisted of using two carbon rods (**Figure 6**) to carry out EIS measurements. Measurements on fixed and dried cells indicated an open-circuit. As a result, the system was developed to **carry out the EIS measurements on live cells**. The real part of the impedance was found to vary nonlinearly from 35 kΩ to few ohms in the range of frequencies considered. This work remains ongoing to determine the effect of UV treatment.

CONCLUSIONS

We demonstrated the complementary information obtained on the same single cells using AFM-based measurements to determine the morphology, nanomechanical, and nanochemical properties. The results shed light on the benefit to consider the different information to improve data collection, analysis, and interpretation. For instance, AFM-IR chemical maps can provide information about the position of the nucleus and other entities inside the cells, which are not always straightforward to detect in the topography images. The results also reveal heterogeneities within the cell and from cell to cell, which should be carefully considered when interpreting the data extracted from selected cells.

A novel aspect of this work is the implementation of single cell analysis using newly developed carbon rods. Single carbon rods were used to acquire I-V curves of different regions of the cells, which confirms the ability to use them as electrodes for electrical measurements. Next, a two-electrode system was designed to carry out EIS measurements on a live single cell. **Implementation of the measurements in liquid is expected to provide an invaluable way to explore the effects of different stressors on single cells in native environmental conditions and expand this multimodal method to encompass electrogenic cells.**

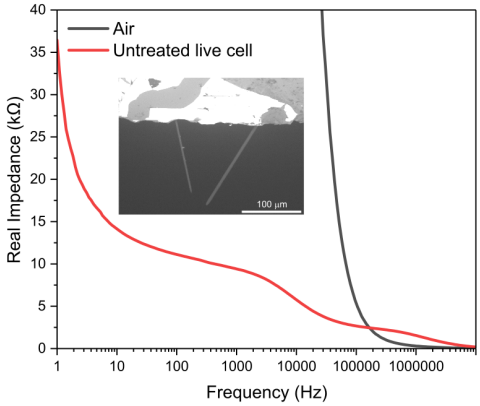

Figure 6: EIS responses of the untreated live fibroblasts (red curve) and air (black curve).

ACKNOWLEDGEMENTS

We acknowledge support from the UCF NanoScience Technology Center. LT acknowledges partial funding from NSF CHE-1847830 and from the Gordon Betty Moore Foundation (10.37807/GBMF11568). Additionally, we would like to thank GSA at UCF and Hilton Head MEMS 2024 workshop for travel funding. All experimental work was carried out at the University of Central Florida.

REFERENCES

1. Stuart, T. and R. Satija, *Integrative single-cell analysis.* Nature Reviews Genetics, 2019. **20**(5): p. 257-272.
2. Heumos, L., et al., *Best practices for single-cell analysis across modalities.* Nature Reviews Genetics, 2023. **24**(8): p. 550-572.
3. Lee, J., D.Y. Hyeon, and D. Hwang, *Single-cell multiomics: technologies and data analysis methods.* Experimental & Molecular Medicine, 2020. **52**(9): p. 1428-1442.
4. Dumitru, A.C. and M. Koehler, *Recent advances in the application of atomic force microscopy to structural biology.* Journal of Structural Biology, 2023. **215**(2): p. 107963.
5. Li, M., *Combining atomic force microscopy with complementary techniques for multidimensional single-cell analysis.* Journal of Microscopy, 2023. **290**(2): p. 69-96.
6. Zemła, J., et al., *Atomic force microscopy as a tool for assessing the cellular elasticity and adhesiveness to identify cancer cells and tissues.* Seminars in Cell & Developmental Biology, 2018. **73**: p. 115-124.
7. Luo, Q., et al., *Cell stiffness determined by atomic force microscopy and its correlation with cell motility.* Biochimica et Biophysica Acta (BBA) - General Subjects, 2016. **1860**(9): p. 1953-1960.
8. Leitner, M., et al., *DNA building blocks for AFM tip functionalization: An easy, fast and stable strategy.* Methods, 2022. **197**: p. 54-62.
9. Li, M., et al. *Imaging and Force Recognition of Single Molecular Behaviors Using Atomic Force Microscopy*. Sensors, 2017. **17**, DOI: 10.3390/s17010200.
10. V. D. dos Santos, A.C., et al., *AFM-IR for Nanoscale Chemical Characterization in Life Sciences: Recent Developments and Future Directions.* ACS Measurement Science Au, 2023. **3**(5): p. 301-314.
11. Mansor, M.A. and M.R. Ahmad, *Single Cell Electrical Characterization Techniques.* Int J Mol Sci, 2015. **16**(6): p. 12686-712.
12. Cheng, L., et al., *Scanning Electrochemical Cell Microscopy Platform with Local Electrochemical Impedance Spectroscopy.* Analytical Chemistry, 2021. **93**(49): p. 16401-16408.
13. Torres-Davila, F.E., et al., *Room temperature 3D carbon microprinting.* Nature Communications, 2024. **15**(1): p. 2745.
14. Mihoubi, W., et al., *FTIR spectroscopy of whole cells for the monitoring of yeast apoptosis mediated by p53 over-expression and its suppression by Nigella sativa extracts.* PLoS One, 2017. **12**(7): p. e0180680.
15. Zhou, J., et al., *A rapid method for detecting conformational changes during differentiation and apoptosis of HL60 cells by Fourier-transform infrared spectroscopy.* Biotechnology and Applied Biochemistry, 2001. **33**(2): p. 127-132.

CONTACT

*Swaminathan Rajaraman, +1 (407) 823-4339, swaminathan.rajaraman@ucf.edu
*Laurene Tetard, +1 (407) 882-0128, laurene.tetard@ucf.edu